Colloids and Surfaces B: Biointerfaces 204 (2021) 111782

Contents lists available at ScienceDirect

Colloids and Surfaces B: Biointerfaces

journal homepage: www.elsevier.com/locate/colsurfb

An injectable double cross-linked hydrogel adhesive inspired by synergistic effects of mussel foot proteins for biomedical application

Zhiwen Zeng [a,b,e,*], Dinghua Liu [c,e], Dejian Li [d,e], Xiumei Mo [a,c,d,e,*]

[a] State Key Laboratory for Modification of Chemical Fibers and Polymer Materials, College of Materials Science and Engineering, Donghua University, Shanghai, 201620, China
[b] Institute of Medicine and Health, Guangdong Academy of Sciences, Guangdong, 510500, China
[c] College of Chemistry, Chemical Engineering and Biotechnology, Donghua University, Shanghai, 201620, China
[d] Department of Orthopedics, Shanghai Pudong Hospital, Fudan University Pudong Medical Center, Shanghai, 201301, China
[e] Shandong International Biotechnology Park Development Co. Ltd, 39, Keji Avenue, Yantai High-Tech Zone, 264670, Shandong Province, China

ARTICLE INFO

Keywords:
Tissue adhesive
Michael addition reaction
Mussel adhesive proteins
Double cross-linked hydrogel

ABSTRACT

Hydrogel adhesives with high tissue adhesion, biodegradability and biocompatibility are benefit for promoting surgical procedures and minimizing the pain and post-surgical complications of patients. In this paper, an injectable mussel inspired double cross-linked hydrogel adhesive composed of thiolated mussel inspired chitosan (CSDS) and tetra-succinimidyl carbonate polyethylene glycol (PEG-4S) was designed and developed. CSDS was synthesized with thiol and catechol groups inspired by the synergistic effect of mussel foot proteins (mfps). The double cross-linked hydrogel was first formed by the addition of sodium periodate (or Fe^{3+}) and then double cross-linked with PEG-4S. The results showed that the mechanical and adhesion properties of the double cross-linked hydrogels were significantly improved by the synergistic effects of the functional groups. And the prepared hydrogels showed good cytocompatibility which evaluated by determining the viability of L929 cells and human umbilical vein endothelial cells (HUVECs). Additionally, the biodegradability and biocompatibility *in vivo* were further confirmed by subcutaneous implantation in mice model, and the histological analysis results identified that the prepared hydrogels were *in vivo* biocompatible. This work presents an injectable mussel inspired double cross-linked hydrogels that can use as a potential hydrogel adhesive for biomedical application.

1. Introduction

The application of tissue adhesives is an effective strategy for bleeding control, wound closure and reconnection of injured soft tissues with much lower cohesiveness, for example, spleen, liver and kidney [1–3]. Fibrin sealant and cyanoacrylate are the two main commercial tissue adhesives for clinical surgical, but they are hampered by the adhesive strength or/and biocompatibility [4]. It was reported that the basic characteristics of an ideal tissue adhesive should include strong adhesion in moisture tissue environment, easy to operate and good biocompatibility, and so on. Currently, hydrogel adhesives have attracted much attention due to their advantages of in situ rapid cross-linkable, injectable, multi-functional, biodegradability and good biocompatibility [5–7]. What's more, it can achieve a significant level of adhesion by various physical or chemical interactions with the specific tissues in the wet environment [8,9]. Literatures have been proved that physical interactions and chemical reaction are important for promoting the adhesion strength of the hydrogel adhesive, such as hydrophobic association, diffusion bond, π−π interaction and Michael addition reaction [10–12]. Therefore, it is important to promote the interfacial interactions between the functional groups of the adhesives and the presence of tissue surface biomolecules with specific functional group [13–15].

Mussel foot proteins (mfps, at least 6 types) are secreted by Marine mussels to enable them to firmly stick to various matrix surfaces under turbulent and salty environment [16,17]. It was believed that 3, 4-dihydroxyphyenylanine (DOPA) that present in mfps is responsible for the exceptional adhesive performance, because the catechol groups of DOPA is participating in various possible physical interactions or chemical reactions, such as π−π interaction, electrostatic interactions, hydrogen

* Corresponding authors at: State Key Laboratory for Modification of Chemical Fibers and Polymer Materials, College of Materials Science and Engineering, Donghua University, Shanghai, 201620, China.
E-mail addresses: zengzwen@sina.cn (Z. Zeng), xmm@dhu.edu.cn (X. Mo).

https://doi.org/10.1016/j.colsurfb.2021.111782
Received 8 February 2021; Received in revised form 16 April 2021; Accepted 20 April 2021
Available online 24 April 2021

bonds, Michael addition reaction and Schiff base reaction [18–20]. Additionally, active *o*-quinone is the oxidized product of DOPA and readily interact with nucleophiles (ex, -NH_2, -SH, or -OH) or coordinate with cations of the surrounding tissues, resulting in strong adhesion to biological tissues [21,22]. Therefore, the DOPA residues group-catechol groups, or its derivative have been utilized to achieve high adhesive property. Meanwhile, it is identified that the other amino acids in mfps, such as glycine, 4-hydroxyarginine, and asparagine cysteine, are also play an important role for the high adhesion in wet environment of Marine mussels [12]. Especially, the high content of thiol groups in the cysteine exhibited the ability to enhance the adhesion properties by controlling the redox chemistry of catechol groups [23,24]. Therefore, the synergistic effects of the functional mfps could promote the adhesive properties of the adhesive plaque.

Further studies proved that the hydrophobic, density of charge and hydrogen bond of the polymer are crucial for enhancing the adhesion properties [25–28]. In this paper, Chitosan (CS) and polyethylene glycol (PEG) were chosen to prepare hydrogel adhesives due to their superior characteristics. Hydrogels based on CS/PEG have been studied in numerous biomedical applications, such as tissue adhesive, hemostatic materials, drug and gene carrier tissue engineering and wound dressing lately [29–31]. CS have abundant amino groups on the backbone due to the partial deacetylation of chitin, and it is a natural positive charged and the second abound polysaccharide with low solubility in liquid solution due to its molecular structure. Additionally, CS is readily functioned with reactive groups or functional polymers [32]. Our previous studies have successful prepared the functional chitosan modified with thiol group and catechol group [33,34]. PEG is a biocompatible, ease in incorporating various functionalities, non-immunogenic and hydrophilic polymer, and it have been utilized for developing biomaterials, biotechnology and medicine [35]. Therefore, CS/PEG based hydrogels are prepared through the physical or chemical reaction strategies and broadly applied in biomedicine.

When hydrogel adhesives are used as tissue adhesives to adhere the trauma tightly, the cohesive of the hydrogel that act as the "glue layer" of adhesive system are also important for the hydrogel adhesive [36,37]. In our paper, inspired by the functions and contributes of mfps, we designed an injectable double cross-linked hydrogel adhesive based on tetra-succinimidyl carbonate polyethylene glycol (PEG-4S) and thiol-grafted mussel inspired catechol conjugated chitosan (CSDS). As seen from Fig. 1, to achieve high adhesive and mechanical strength, the double cross-linked hydrogels were prepared by the sequential two-step cross-linking procedure. The first cross-linked network was formed by the catechol groups with the addition of sodium periodate ($NaIO_4$) or $FeCl_3$ solution, and the second cross-linked network was formed by the reaction between thiol group and succinimidyl carbonate ester through Michael addition reaction. The gelation time, equilibrium water content, *in vitro* degradation, morphology, mechanical properties and adhesive properties of the hydrogel adhesives were evaluated. In addition, MTT assay and CCK-8 assay was used to determine the viability of L929 cells and human umbilical vein endothelial cells (HUVECs), respectively. Furthermore, *in vivo* biodegradation and biocompatibilities of the prepared hydrogel adhesives were also studied by subcutaneous implantation in mice model. This double cross-linked hydrogel adhesive system may be useful for a wide range of biomedical applications.

2. Experimental section

2.1. Materials

Chitosan (CS, medium molecular weight, with an 85 % nominal degree of deacetylation) and N-acetyl-L-cysteine (NAC) were purchased from Sigma-Aldrich. 1-(3-Dimethylaminopropyl)-3-ethylcarbodiimide hydrochloride (EDC•HCl), sodium periodate and 4-(Dimethylamino) pyridine (DMAP) were from Sinopharm Chemical Reagent Co., Ltd. 4-arm polyethylene glycol (4-arm-PEG, 10000 Da) was purchased from Creative PEGWorks company. 3,4-dihydroxyhydrocinnamic acid was brought from Energy Chemical company. N, N'-Disuccinimidyl carbonate (DSC) was brought from Shanghai Wo Kai Co., Ltd. 3-(4,5-dimethylthiazol-2-yl)-2,5diphenyltetrazolium bromide (MTT) and CCK-8 were from Biosharp, Fetal bovine serum (FBS) and Trypsin-EDTA (0.25 %) were bought from Gibco, Dulbecco's modified eagle medium (DMEM, high glucose), RPMI culture medium, Penicillin (1000 units/mL) and streptomycin (1000 μg/mL) solution were from Hyclone. Other chemical reagents were from Sinopharm Chemical Reagent Co., Ltd and used as received.

2.2. Synthesis of PEG-4S

PEG-4S was synthesized as the literature description [38]. 4-arm PEG (0.40 mmol) was dissolved in 30 mL of dry dioxane (molecular sieve) with under stirring at 60 °C. The clear solution was then cooled to room

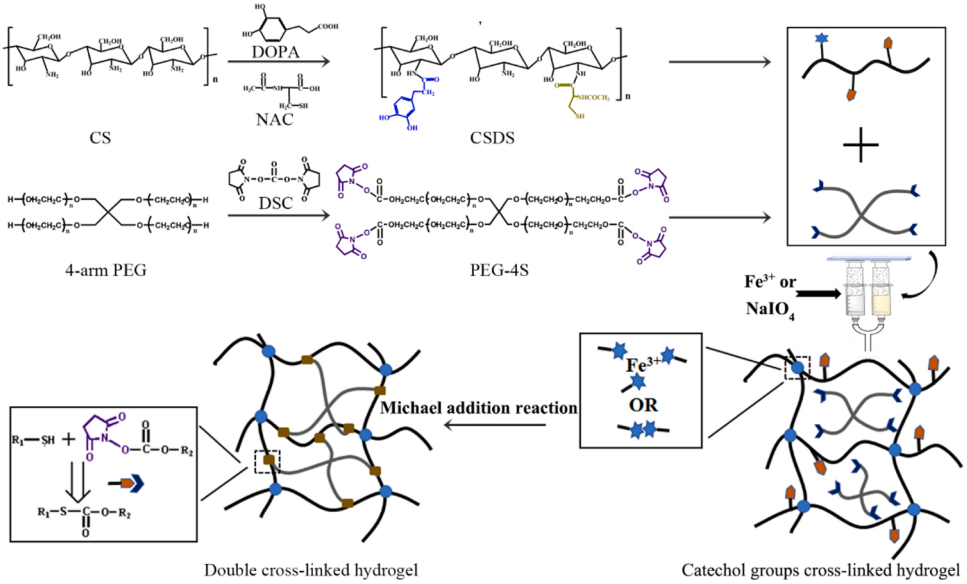

Fig. 1. Schematic of the preparation of the injectable double cross-linked hydrogel adhesive composed of PEG-4S and CSDS. Firstly, hydrogel was rapid formed by the reactions between catechol groups and Fe^{3+} or $NaIO_4$, and then the double cross-linked hydrogel was prepared by the reactions between PEG-4S and thiol groups.

temperature. DSC (4.0 mmol) in 10 mL of dry acetone and DMAP (4.0 mmol) in 10 mL of dry acetone were added slowly under stirring. Reaction proceeded for 8 h at room temperature. After 8 h, the reaction solution was precipitated into excess cold diethyl ether. To purify the product, it was re-dissolved in acetone, and precipitated in ether, this cycle was repeated three times.

2.3. Thiolation of bio-inspired catechol conjugated chitosan (CSDS)

The synthesized CSDS was obtained by two steps carbodiimide coupling method. Firstly, catechol conjugated chitosan (CS-dopa) was synthesized. Typically 1.0 g of CS was dissolved in 100 mL of acetic acid (pH = 5.0) under stirring for 30 min, then 15 mL of 3,4-dihydroxyhydrocinnamic acid (3.44 mmol) solution was added to the CS solution, subsequently 30 ml EDC•HCl (10.32 mmol) solution with 1:1 v/v mixture of water and ethanol was added. Reaction proceeded for 24 h at room temperature under stirring. The pH of the reaction solution was controlled at 4–5 during the reaction period. After 24 h, the solution was dialyzed against ultrapure water for 3 days and lyophilized. The lyophilized product was CS-dopa.

Secondly, 0.5 g of CS-dopa was added into the bottle containing 50 mL of ultrapure water and dissolved under stirring by adjusting the pH to 5.0. Then 5.16 mmol NAC was added to the CS-dopa solution followed by the addition of 10.32 mmol EDC•HCl. Reaction proceeded for 12 h under stirring at room temperature, the pH value of the solution was controlled at 4–5. After 12 h, the reaction solution was transferred into the dialysis tube (MWCO: 10000 DA) to dialyze against ultrapure water for 3 days, and then lyophilized. The obtained product was CSDS.

2.4. Characterization of PEG-4S and CSDS

To confirm the synthesis of 4-arm PEG-4S and CSDS, Attenuated Total Reflection Fourier transform infrared spectroscopy ((ATR-FTIR) was used to test the sample in the wavenumber range of 600 − 4000 cm^{-1}. Additionally, PEG-4S and CSDS were dissolved in deuterated chloroform ($CDCl_3$) and deuterated heavy water (D_2O), respectively, and then measured on Bruker NMR spectrometer (600 MHz), the substitute degree of succinimidyl carbonate ester was calculated by the ^1H NMR spectra of PEG-4S. Furthermore, the quantities of catechol groups and thiol groups grafted onto CSDS were determined by Waite and Benedict's test [39] and Ellman's test, respectively. To calculate the contents of thiol groups and catechol groups in CSDS, the standard curve at 412 nm to thiol groups and standard curve at 500 nm to catechol groups were established with known standard sample concentration.

2.5. Preparation and gelation of the double cross-linked hydrogels

To prepare the hydrogels, 4% (g/mL) CSDS solution and 60 % (g/mL) PEG-4S precursor solution was prepared respectively. Then the two solutions were mixed in one syringe of the dual-syringe injector, the other syringe was added with the fast cross-linker (10 μmol/L $NaIO_4$ or 20 μmol/L $FeCl_3$ solution), subsequently hydrogels were prepared by pushing the solutions from the dual-syringe injector and then placed in an incubator for 3 h at 37 °C to complete the covalent cross-linking with PEG-4S, thus the double cross-linked hydrogels were prepared. The double cross-linked hydrogel that containing $NaIO_4$ was denoted as CSDS-P-I, and that containing Fe^{3+} was denoted as CSDS-P-Fe. Two types of single cross-linked hydrogels, CSDS-P and CSDS-Fe was also prepared, CSDS-P was prepared by placing the CSDS and PEG-4S solution into the incubator for 3 h, and CSDS-Fe was prepared by adding $FeCl_3$ solution into CSDS solution. The molar ratio of thiol group (-SH) to succinimidyl carbonate group was 1:1, $NaIO_4$ to catechol group was 0.75:1, and Fe^{3+} ion to catechol group was 1:3.

To study the gelation process of the hydrogel adhesive, three cross-linkers, 60 % (g/mL) PEG-4S solution, 10 μmol/L $NaIO_4$ or 20 μmol/L $FeCl_3$ solution was mixed with equal volume of 4% CSDS solution, and then formed 2%CSDS-P, 2%CSDS-Fe, and 2%CSDS-I hydrogels, respectively. The time-sweep experiments were performed to monitor the gelation time of 2%CSDS-P, 2%CSDS-Fe, and 2%CSDS-I hydrogels at 25 °C by using a rotating rheometer (ARES-RFS, TA Instruments). The frequency was set at 1.0 Hz and strain was set at 5%.

2.6. Morphological observation, swelling properties and in vitro degradation

The internal morphologies of the prepared hydrogels were observed via scanning electron microscope (SEM, Phenom XL, Phenom World, the Netherlands). Before SEM observation, all samples were lyophilized and exposed the internal structure, and then coated with platinum for 30 s to observe. To assess the equilibrium water content and *in vitro* degradation, disc-shaped samples (diameter = 12 mm, thickness = 2.5 mm) were prepared. The prepared hydrogels (n = 5) for equilibrium water content testing were lyophilized to measure the weight of dry hydrogel (*Wd*), and then, samples were immersed in PBS solution (pH = 7.4) and incubated for 24 h at 37 °C. The swelling equilibrium samples were weighed (*Ws*). The equilibrium water content (EWC) of hydrogel was calculated as follows:

$$\mathrm{EWC(wt\%)} = \frac{W_s - W_d}{W_s} \times 100\% \quad (1)$$

Where *Ws* is the weight of the swelling equilibrium hydrogel, *Wd* is the weight of the dry hydrogel.

The *in vitro* degradation of hydrogel adhesives (n = 3) was also measured by weighing methods at predetermined time points. The hydrogels were incubated in PBS solution (pH = 7.4) at 37 °C. The initial time of the hydrogel degradation was taken at the point when the weight (*Wi*) reached the swelling equilibrium. The degraded hydrogel samples were measured at predetermined time intervals after removal the additional PBS solution, and these values were recorded and denoted as *Wt*. The PBS solution were refreshed after the testing hydrogels were weighed. The remaining weight ratio of testing hydrogels was calculated as follows:

$$\text{Remaining weight ratio(wt\%)} = \frac{W_t}{W_i} \times 100\% \quad (2)$$

Where *Wt* is the weight at time t of the testing hydrogel and *Wi* is the initial weight of the testing hydrogel.

2.7. Rheological experiment

The rheological measurements of samples were performed by using a rotating rheometer (ARES-RFS, TA Instruments) equipped with 25-mm stainless steel parallel plate. CSDS-Fe, CSDS-P, CSDS-P-Fe and CSDS-P-I hydrogels were fresh prepared as described in 2.5 section of this paper and they were incubated for 3 h at 37 °C to complete the cross-linking reaction. After the testing sample was placed on the lower plate of the rheometer, the upper plate was carefully lowered to a gap size (~1 mm), then measurement started. The testing hydrogel was analyzed under oscillatory dynamic strain analysis first in order to ensure the liner viscoelastic of the rheological measurement, for the oscillatory dynamic strain analysis, the measured frequency was 1.0 Hz, and the strain was increased from 0.1%–100%. Finally, the strain was 5% for the frequency sweep measurement. Then the testing data of elastic modulus (G', solid-like behavior) and loss modulus (G", liquid-like behavior) were recorded by conducting dynamic frequency analysis in the range of 0.1–100 rad/s. All the experiments were operated at 25 °C.

2.8. Measurement of adhesion strength

The adhesion strength of hydrogel adhesives was analyzed by lap shear testing and pork skin was used as adherend. Fresh pork skin purchased from local slaughterhouse was scraped off the abound fat under the dermal tissue. Then rectangular pork skins (10 mm × 30 mm) were prepared for testing. The CSDS and PEG-4S solution was applied to the rectangular pork skin, and covered with the other rectangular piece of pork skin containing fast cross-linker ($NaIO_4$ or Fe^{3+}), the overlapping area was maintained 10 mm × 10 mm and the hydrogel adhesive was cured rapidly. For a comparative study, adhesion strength of the single cross-linked hydrogel adhesives, CSDS-Fe and CSDS-P, were also tested. Samples were stored in a incubator for 30 min or 3 h at room temperature, then the adhesiveness of hydrogel adhesive was evaluated by using a universal tensile testing machine (HY-940FS, Shanghai Hengyu Co., Ltd) and the moving speed was set at 5 mm per minute.

2.9. In vitro cytotoxicity test

The cytotoxicity of the adhesives was studied according to ISO 10993-5 standard test method. MTT assay and CCK-8 assay were used to determine the viability of L929 cells and HUVECs, respectively. The hydrogel samples were sterilized by using 75 % ethanol for 5 h and then washed 3 times with PBS solution to remove the ethanol. Subsequently, samples were moved to the centrifuge tube containing 20 mL DMEM and the concentration was 5.0 mg/mL, then they were incubated in the incubator set at 37 °C and 100 rpm for 24 h. The extractions were prepared by filtration (filter diameter = 0.22 μm). Then 10 % fetal bovine serum (FBS) and 1% of penicillin and streptomycin (pen/strep) solution were added into the extractions for the cytotoxicity test. 100 microliters 1.0×10^5 cells/mL L929 cells suspensions were pipetted into 48-well culture plates. The plates were transformed to the cell incubator under standard culture conditions at 37 °C and 5% CO_2. After 24 h, the medium of the plates was replaced with the prepared extractions, and cultured for a predetermined time interval in the cell incubator. Additionally, L929 cells cultured with fresh culture medium was regard as the negative control. Thereafter, the culture medium of the measurement was removed at the predetermined time, and 200 μL of DMEM supplemented with 20 μL MTT solution (5 mg/mL) was pipetted into each well and incubated for another 4 h. The culture medium with unreacted MTT was replaced by adding 200 μL of dimethyl sulfoxide and dissolved the forming formazan crystal for 15 min at 37 °C. ELISA microplate reader (Multiscan GO, Thermo Scientific) was used to measure the optical density values at a wavelength of 570 nm.

The CCK-8 assay was also performed to evaluate the cytotoxicity of the hydrogel extractions on HUVECs, and the experimental operation was similarity to MTT assay. Briefly, HUVECs were seeded in 48-well cell culture plates at a density of 1.0×10^4 cells per well and cultured for 24 h in RPMI culture medium, then it was replaced with hydrogel adhesive extractions. The extractions were removed at predetermined time point (24 h, 48 h, and 72 h), and replaced with a mix solution of 200 μL of CCK-8 in RPMI culture medium. After the plates were incubate for another 2 h, the optical density values were measured at the wavelength of 450 nm using ELISA microplate reader (Multiscan GO, Thermo Scientific). HUVECs were seeded to the fresh culture medium as the negative control.

2.10. In vivo study

To assess the degradation behaviors and biocompatibility of the prepared hydrogels *in vivo*, CSDS-Fe, CSDS-P, CSDS-P-Fe and CSDS-P-I hydrogels subcutaneously implanted in the backs of ICR mice. All animal studies were performed in compliance with guidelines set by national regulations and approved by the local animal experiments ethical committee. ICR mice (Male, 200 g, Jiesijie Laboratory Animal Co. Ltd, Shanghai, China) was anesthetized by sodium pentobarbital (30 mg/kg). After their back were shaved, a skin incision 2.0 cm long and enough skin thickness deep was made for implanting hydrogel sample. Then the prepared weighed hydrogels were subcutaneously implanted and incisions were closed by suture quickly. ICR mice were euthanasia at predetermined time intervals and the implantation sites with the samples were harvested. For *in vivo* degradation assessment, the hydrogel adhesive explants were carefully dissected from surrounding skin tissue and weighed after remove the tissues on the surface. The average weight of sample before implanted was defined as the initial weight (W_0) and assigned a value of 1.0. The remaining weight (Wr) of sample on day 5 and 10 were normalized to W_0, therefore, the remaining weight ratio (%) = Wr/W_0. Photographs of the remaining hydrogels were obtained with a digital camera. For histological evaluation, skin tissues were fixed in 10 % (g/mL) formaldehyde solution, and stained using hematoxylin and eosin (H&E) and Masson's trichrome staining for analyzing the degree of tissue response, typically inflammation and fibrosis.

2.11. Statistical analysis

Statistical analysis was conducted by using Origin 8.0 software with one-way analysis of variance (ANOVA), followed by a Bonferroni test. It was considered statistically significant when p-value < 0.05.

3. Results and discussion

3.1. Synthesis and characterization of the functional PEG-4S and CSDS

In our study, we have designed and prepared a double cross-linked hydrogel adhesive composed of PEG-4S and CSDS, and the synthesized PEG-4S and CSDS were identified by ATR-FTIR, ^{1}H NMR and UV–vis spectroscopy (Fig. 2 and Fig. S1, Supporting Information). The PEG-4S was synthesized by grafting the succinimidyl carbonate ester onto the chain end of PEG via esterification reaction (Fig. S2, Supporting Information). As shown in Fig. 2A, compared to PEG, PEG-4S showed a new band at 1715 cm^{-1} which could be assigned to the ester bond, and the ^{1}H NMR spectra have further studied to confirm the existence of succinimidyl carbonate ester. In Fig. 2C, the multiple peaks at 3.98−3.36 ppm were assigned to the methylene protons of the PEG backbone, while the single peak at 8.32 ppm belong to the methylene protons of succinimidyl carbonate ester. The substitute degree of succinimidyl carbonate ester in PEG-4S was about 75 % that calculated according to the integral area of ^{1}H NMR spectra.

The mussel inspired CSDS was synthesized by functioned CS with catechol group and thiol group via EDC/NHS chemistry, and the synthetic route of CSDS was shown in Fig. S3 (Supporting Information). The chemical structure was confirmed by ATR-FTIR and ^{1}H NMR, as shown in Fig. 2B and D. In Fig. 2B, the new band at 3112 cm^{-1} was assigned to the stretch vibrations of S—H, and the band at 1640 cm^{-1} was assigned to the C═O stretch vibrations of amide bond, and the intensity of CSDS was higher than CS. The ^{1}H NMR spectra of CSDS further confirmed the catechol group and thiol group grafted onto the backbone of CS (Fig. 2D). Compared with CS-Dopa, the peaks of CSDS at 7.32−7.03 ppm were assigned to protons of phenyl group, while the peaks of CS-Dopa assigned to protons of phenyl group was showed at 6.82−6.52 ppm, and the peak at 4.49 ppm can be assigned to protons of methylene group (marked with an asterisk) close to phenyl group in dopamine, the peak at 3.55 ppm can be assigned to protons of methyne group of NAC, the peaks at 2.06−1.70 ppm were assigned to the protons of methylene group close to the thiol group, the peaks at 0.93−0.61 ppm were assigned to the protons of methyl group of NAC. The content of catechol groups and thiol group in the CSDS was 100 μmol/g and 400 μmol/g, respectively, which were calculated from the established standard curves (Fig. S1, Supporting Information).

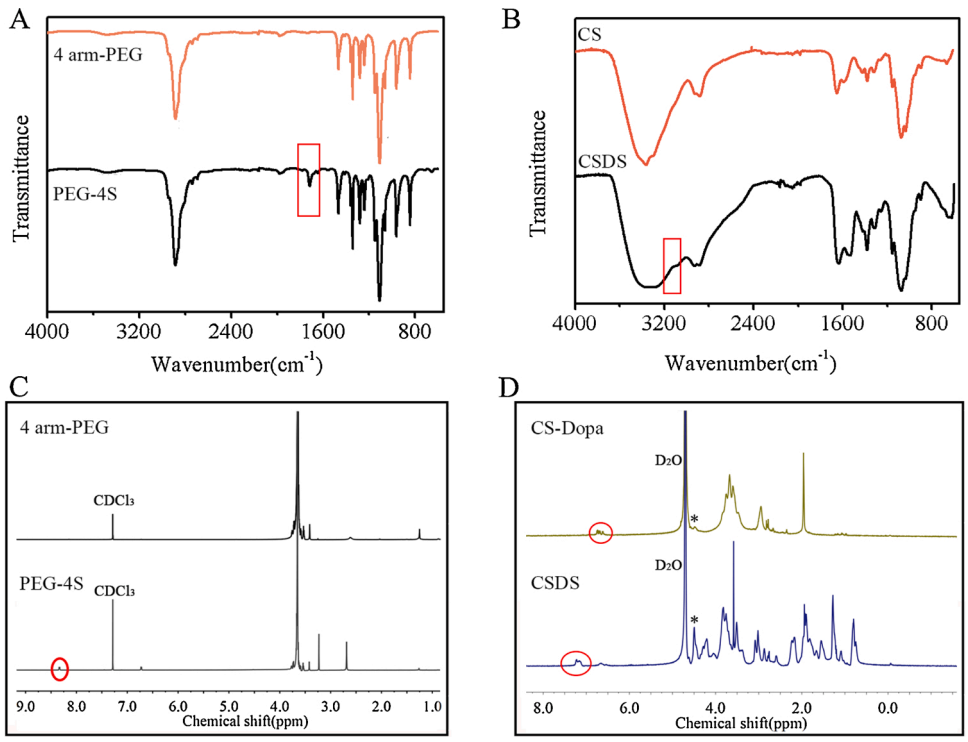

Fig. 2. The FTIR spectra and ^{1}H NMR spectra of the synthesized PEG-4S and CSDS.

3.2. *Preparation and characterization of injectable hydrogel adhesives*

In this paper, two types of double cross-linked hydrogels, CSDS-P-Fe and CSDS-P-I were prepared. $NaIO_4$ or Fe^{3+} ion was designed as the fast cross-linker, while PEG-4S was designed as the slower cross-linker. It was reported chitosan was hard to dissolve in the liquid water or PBS solution, however, the solubility would be promoted by grafting catechol group and thiol group [31,40]. Therefore, to prepare the hydrogels, the flowing CSDS/PEG-4S solution was injected from the dual-syringe injector, meanwhile, the fast cross-linker was also injected from the other syringe of the dual-syringe injector. As illustrated in Fig. 3A, B and C, the gelation time of 2% CSDS with $NaIO_4$, Fe^{3+} ion or PEG-4S was evaluated by using a rotating rheometer. The crossover points of elastic modulus (G') and loss modulus (G") was usually regarded as the onset of gelation. It was showed that the gelation time of the 2%CSDS-Fe and 2% CSDS-I were less than 1 min due to the rapid cross-linking reaction. The

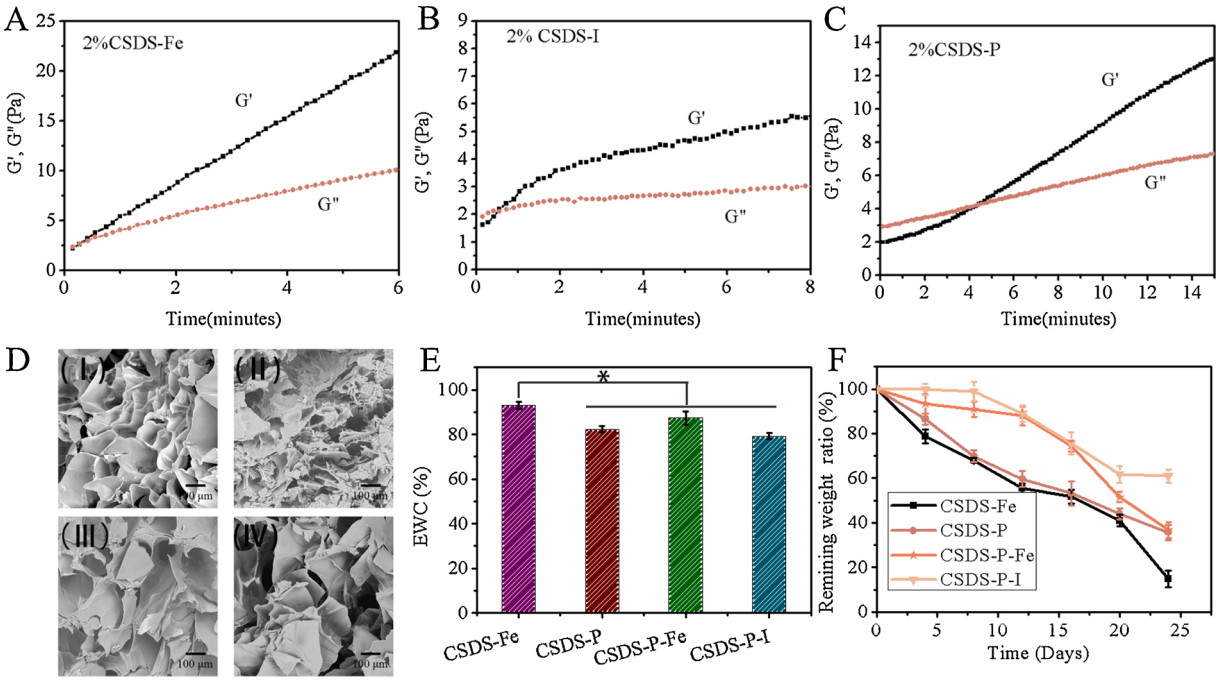

Fig. 3. The gelation time of (A) 2%CSDS-Fe, (B) 2%CSDS-I, (C) 2%CSDS-P. (D) The representative SEM image of hydrogel morphology: (I) CSDS-Fe (II) CSDS-P, (III) CSDS-P-Fe, (IV) CSDS-P-I. (E) The EWC of CSDS-Fe, CSDS-P, CSDS-P-Fe and CSDS-P-I. (F) The degradation test of CSDS-Fe, CSDS-P, CSDS-P-Fe and CSDS-P-I. "*": p-value<0.05, it was considered statistically significant.

2%CSDS-Fe hydrogel was the fastest of all, which was formed via forming catechol-Fe^{3+} complexes (bis- or tris-, Fig. S4, Supporting Information), and the gelation time of 2%CSDS-I hydrogel was a bit longer than 2%CSDS-Fe hydrogel due to the oxidation of catechol groups (Fig. S5, Supporting Information). Additionally, the gelation time of 2% CSDS-P hydrogel was about 4.5 min that was much longer than the others. The gelation time of the double cross-linked hydrogels also tested and the results showed it was similarity to the single cross-linked hydrogels (Fig. S6, Supporting Information). Thus, for the double cross-linked hydrogels, the Michael addition reaction between thiol groups of CSDS and succinimidyl ester of PEG-4S was cross-linked to form the second network structure (Fig. S7, Supporting Information).

As presented in Fig. 3D, the inner morphologies of CSDS-Fe, CSDS-P, CSDS-P-Fe and CSDS-P-I were observed by SEM. It was showed the morphology and porosity of the hydrogel network were dependent on the cross-linked density. For example, CSDS-Fe hydrogel network showed the loose sponge-like structure with biggest pore diameter. With the addition of PEG-4S to form double cross-linked hydrogel, the pore diameter of the CSDS-P-Fe hydrogel network tended to be smaller than the single cross-linked hydrogel network. As shown in Fig. 3E, The EWC of CSDS-Fe was about 93 % that was the most of all the testing samples. CSDS-P-I hydrogel contained least water, and its EWC was about 79 %. Compared to CSDS-Fe hydrogel, the EWC of the other CSDS-P, CSDS-P-Fe and CSDS-P-I was significant lower. The *in vitro* degradation of the prepared hydrogels was also evaluated (Fig. 3F). The results showed that the prepared hydrogels were degradable, and the degradation rate was dependent on the cross-linker. After 24 days, the remaining weight ratio of CSDS-Fe hydrogel was less than 20 % while CSDS-P-I hydrogel was about 60 %, it proved that the double cross-linked hydrogel was more stable, and the CSDS-Fe hydrogel easily broke down and degraded.

3.3. Analysis of mechanical properties

The rheological studies were conducted to characterize the mechanical properties of the prepared hydrogels. Hydrogels showed both liquid-like properties (loss modulus, G") and solid-like behaviors (storage modulus, G'). At first, dynamic strain analysis was used to analyze the hydrogels to decide the liner viscoelastic of the prepared hydrogels (Fig. S8, Supporting Information). As can be seen, the G' values of CSDS-P-Fe and CSDS-P-I hydrogels were bigger than CSDS-Fe and CSDS-P due to the high cross-linking density of double cross-linked hydrogels. However, The G' values of CSDS-P hydrogel was going down at high shear strain, which indicated that the network structure of CSDS-P broke down. Based on these data, 5% strain was determined for dynamic frequency sweep analysis of the hydrogel samples which performed to study the mechanical strength, and the results were displayed in Fig. 4. The G' of CSDS-P-Fe was increased from 690 Pa at 0.1 rad/s to 900 Pa at 100 rad/s. Compared with CSDS-Fe and CSDS-P hydrogels, the double cross-linked hydrogels showed higher values of G', which means that the mechanical strength of double cross-linked hydrogels was higher. In addition, the G' of CSDS-P-I was the highest of all the testing samples that was reached up to 1100 Pa, and G' of CSDS-P was the lowest that ranged from 180 Pa to 300 Pa, when the testing frequency was analyzed between 0.1 and 100 rad/s. It is noteworthy that the mechanical strength of CSDS-P-I was higher than CSDS-P-Fe due to the generation of covalent bond of CSDS-P-I, and CSDS-Fe hydrogel showed higher values of loss modulus (G") than the other prepared hydrogels which indicate that it was softer at lower frequencies. The results indicated that polymer network was important for the viscoelastic behaviors of hydrogels, and the viscoelastic behavior was controlled primarily by the nature of imposed mechanical motion and the flexibility of chains.

3.4. Evaluation of adhesion properties

Adhesion strength of the prepared hydrogels was evaluated by lap shear test that used porcine skin as an adherend (Fig. 5A). Porcine skin with biological similarity to human dermis was commonly used for various biomedical experiments. As seen from the Fig. 5B and C, the adhesion strength of double cross-linked hydrogels was bigger than the CSDS-Fe and CSDS-P hydrogels. After incubated for 30 min, CSDS-P-I showed the largest adhesion strength which was 53.32 ± 3.53 kPa, it was much larger than other mussel inspired hydrogel adhesives that reported [29–31]. The adhesion strength of CSDS-Fe was the smallest of all the prepared hydrogels which was 26.62 ± 3.12 kPa, but it was a

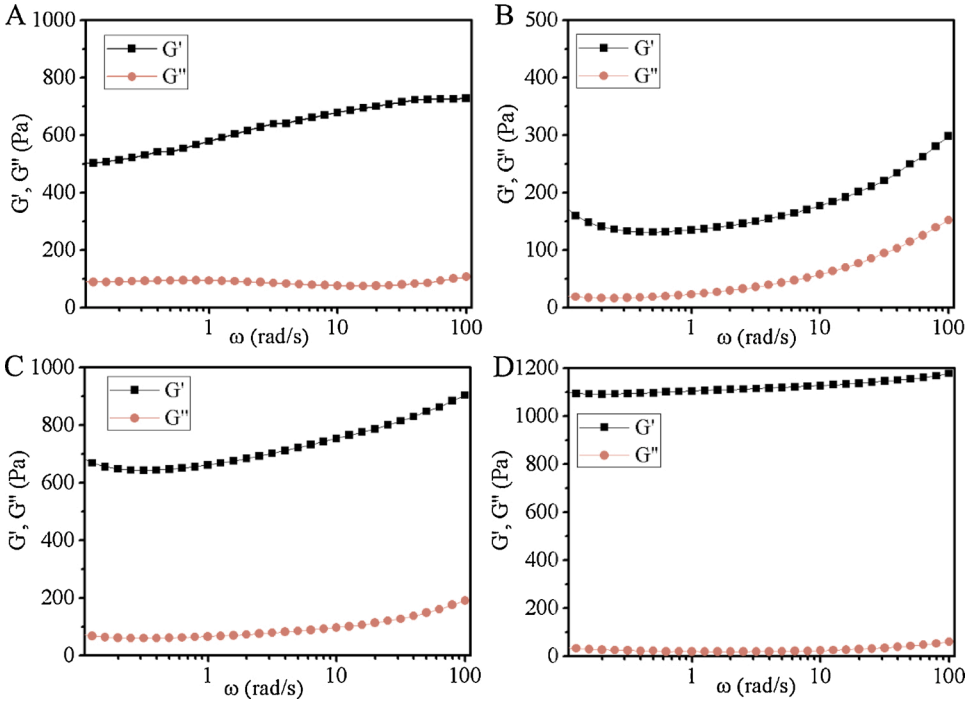

Fig. 4. Storage modulus (G') and viscous modulus (G") of the prepared hydrogels were measured by performing dynamic frequency sweep between 0.1 and 100 rad/s: (A) CSDS-Fe, (B) CSDS-P, (C) CSDS-P-Fe, (D) CSDS-P-I.

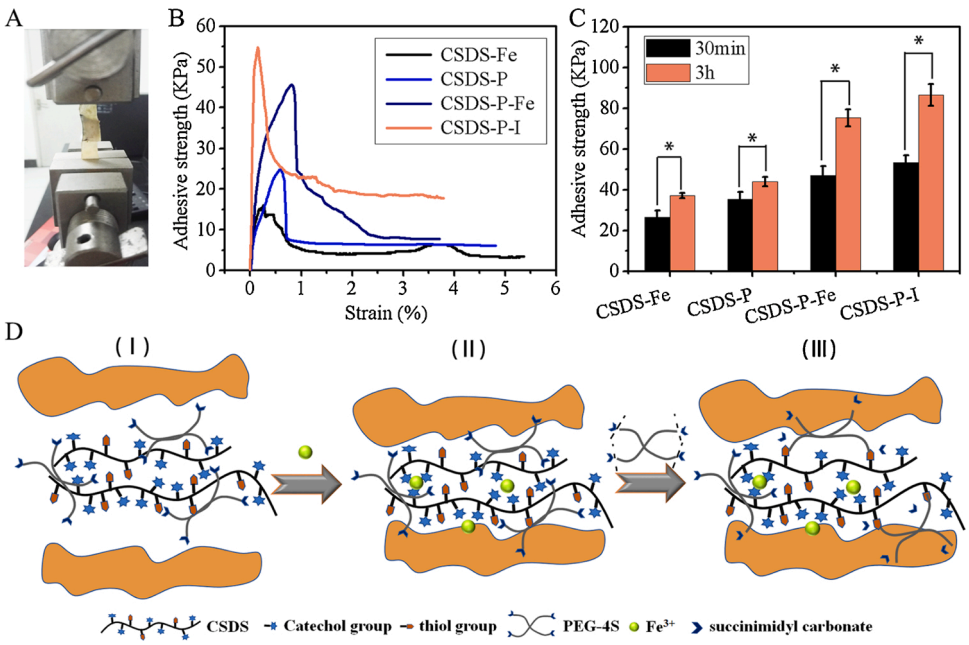

Fig. 5. (A) Adhesion strength of the prepared hydrogels was evaluated by lap shear test. (B) The representative adhesive strength-strain curves of the hydrogel adhesives. (C) The adhesive strength of CSDS-Fe,CSDS-P, CSDS-P-Fe and CSDS-P-I hydrogels incubated for 30 min and 3 h, respectively. (D) The double cross-linked hydrogel was formed by the reaction of groups with cross-linker, meanwhile they were also bonding with the surrounding tissues through various interactions.

little higher than ~25 kPa of fibrin glue reported by Dongyeop X. Oh [41]. Furthermore, the adhesion strength of hydrogel adhesives was significant increasing after incubated for 3 h when compared with samples incubated for 30 min, especially for the double cross-linked hydrogel adhesives. For example, after incubated for 3 h, the adhesion strength of CSDS-P-Fe and CSDS-P-I was increased from ~46 kPa and ~53 kPa to ~75 kPa and ~86 kPa, respectively, while the adhesion strength of CSDS-Fe and CSDS-P was increased from ~26 kPa and ~35 kPa to ~37 kPa and ~43 kPa, respectively. It is notable that the adhesion strength of CSDS-P-I was higher than CSDS-P-Fe due to covalent bond generated by the oxidation reaction. The result showed that the adhesion strength was enhanced by the formation of double cross-linked network and the reactive groups, such as catechol groups, thiol groups, and reactive succinimidyl ester, and the controlling of redox reaction between thiol groups and catechol groups was also play an important role due to storing the catechol groups. On one hand, these groups were reacted to form double cross-linking networks to enhance the mechanical properties, on the other hand, they were bonding with the surrounding tissues through various interactions that reacted with the specific functional groups (ex, -NH_2, -SH, -OH, -COOH) within surrounding tissues (Fig. 5D). Therefore, considering the synergistic effects of the reactive groups and mechanical strength of hydrogels, the prepared double cross-linked hydrogel exhibited high adhesive strength.

3.5. *In vitro* cytocompatibility

For hydrogel adhesives, except the high adhesive properties, biocompatibility is one of the most important properties. *In vitro* cytocompatibility was evaluated to study the biocompatibility of the double-cross-linked hydrogels. It was carried out by determining cellular growth and survival of L929 cells and HUVECs using MTT assays and CCK-8 assays, respectively. As shown in Fig. 6A, L929 cells cultured in the prepared hydrogel extractions and negative group (fresh culture medium) showed significantly proliferation with the culture time increasing from 24 h to 72 h. Compared to the negative group, L929 cells cultured in hydrogel extractions showed lower cell viabilities after 24 h

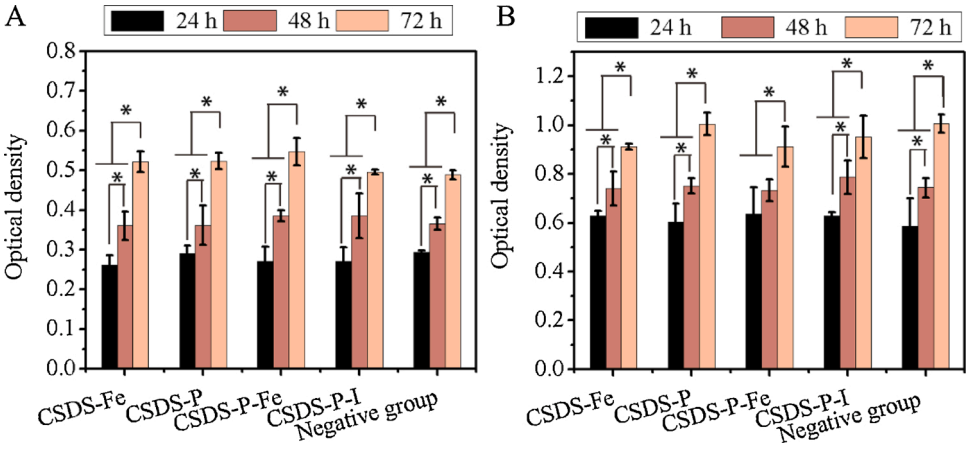

Fig. 6. (A) Cytotoxicity of the prepared hydrogel extractions on L929 was evaluated by MTT assays. (B) Cytotoxicity of the prepared hydrogel extractions on HUVECs was evaluated by CCK-8 assays.

while it was higher after 72 h. Furthermore, at the same cultured time point, the cell viability of L929 cells cultured in different hydrogel extractions was unequal, but the statistical analysis proved the difference of them was not statistically significant. It was indicated that the hydrogel samples (CSDS-P-I, CSDS-P-Fe, CSDS- Fe and CSDS-P) had almost no negative impact on the L929 cells.

The *in vitro* good cytocompatibility of the prepared hydrogels was validated via determining the HUVECs viability by CCK-8 assays. As can be seen from Fig. 6B, the cultured HUVECs were significant proliferated with the increasing cultured time. The statistical analysis result showed that the testing optical density of HUVECs cultured in the prepared hydrogel extractions was close to the negative group, and the difference of the cell viability was not statistically significant at the same culture time. Previous literatures have reported that reactive oxygen spices that harm to cells were generated during the catechol oxidation process [42]. However, this paper showed the mussel inspired hydrogels was nontoxic to the cells, it may be contributed to the special redox mechanism of thiol group to catechol group [23,24]. Therefore, both the MTT assays and CCK-8 assays showed the double cross-linked hydrogel adhesive was a good cyto-compatible biomaterial.

3.6. *In vivo degradation*

Fresh cylindrical hydrogel samples were subcutaneously implanted in the back of ICR mice in order to preliminarily assess the degradation *in vivo* and biocompatibilities (Fig. 7A). The degradation ratio *in vivo* and the degree of the tissue responses to the prepared hydrogel implants were evaluated over the implantation time. The residual implanted hydrogels were dissected from the tissues after implanted for 5, 10, 15 days, and the obtained hydrogel samples was evaluated using a digital camera and weighed by the analytical balance, as shown in Fig. 7B and C. Fig. 7B showed the typical global images of the hydrogels before and after implantation on days 5, 10. It was showed the size of hydrogels were dropped after being subcutaneously implanted. The hydrogels were not break into pieces, so the *in vivo* degradation of the samples was seemed to be controlled by the surface erosion. To assess the degradation more clearly, *in vivo* degradation of the hydrogels was quantified by measuring the residual implanted hydrogels weights, and the results was showed in Fig. 7C. After 5 days implantation, the remaining ratio of CSDS-P-I was ~55 % which was the largest while the remaining ratio of CSDS-Fe, CSDS-P and CSDS-P-Fe were ~34 %, ~39 % and ~45 %, respectively. Samples were degraded fast after 5 days implantation because of the big contact area with the surrounding tissues, the degradation rate was dropped. The degradation ratio of double cross-linked hydrogels (CSDS-P-I < CSDS-P-Fe) were lower than the single cross-linked hydrogels (CSDS-P < CSDS-Fe), and the remaining weight of CSDS-P-I (~29 %) was the biggest of all the samples after implantation on days 10. In addition, after 10 days implantation, the remaining ratio CSDS-Fe, CSDS-P and CSDS-P-Fe was ~19 %, ~21 % and ~24 %, respectively. The *in vivo* degradation of hydrogels was faster than the *in vitro* degradation of hydrogels (Fig. 3F) due to the complex body liquid containing enzymes and other chemical spices that promoting the degradation. And at day 15, the microscope size of prepared hydrogel was not observed, which indicated that the hydrogels could be thoroughly degraded *in vivo*, and the degradation rate was consistent with that needed for skin healing phases I–II (2–3 weeks) [43].

3.7. *Histological evaluation*

The histological sections of the tissues attached to the hydrogels were harvested and stained with H&E to further evaluate the biocompatibility. As shown in Fig. 8, after implanted in subcutaneous tissue of ICR mice for 5 days, 10 days and 15 days, the H&E staining images were obtained to study the effect of implantation materials and its degradation products on tissue response. Because the component CSDS of hydrogel was bearing positive charges, the hydrogels displayed red in the H&E staining images. After 5 days of implantation, some inflammatory cells containing a major part of nuclei and small contents of

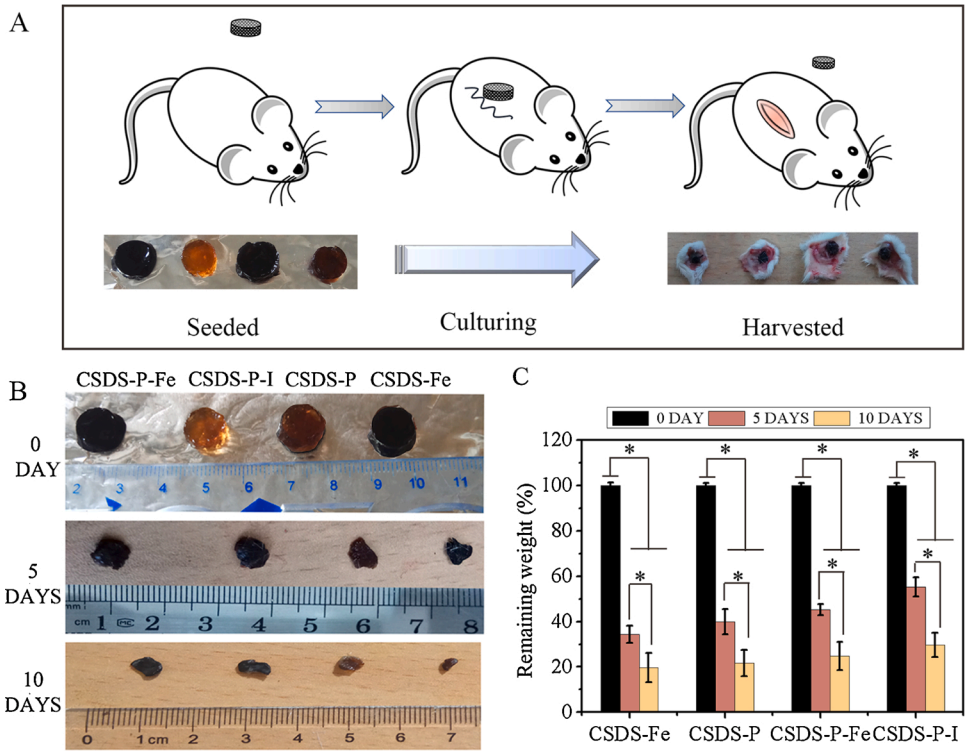

Fig. 7. *In vivo* degradation of 4%CSDS- P-Fe, 4%CSDS-P-I, 4%CSDS-Fe and 4%CSDS-P hydrogels using a rat subcutaneous model on days 0, 5 and 10 of implantation. (A) Schem of subcutaneously implantation of the cylindrical hydrogel samples in the back of ICR mice. (B) Representative images and (C) remaining weight ratio of the implanted hydrogels.

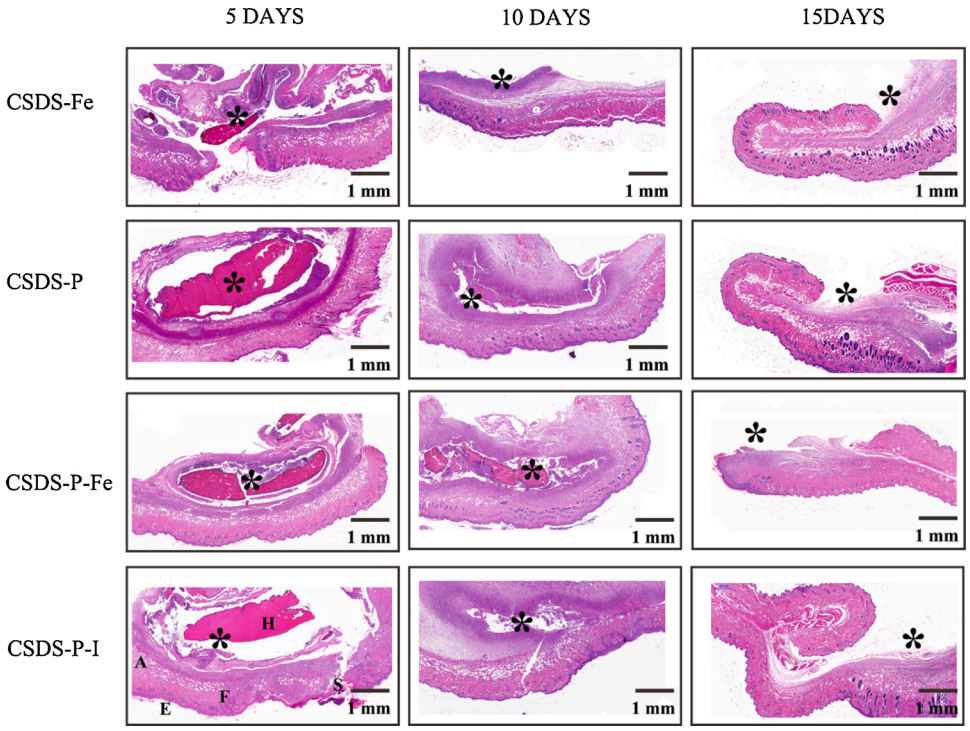

Fig. 8. H&E staining images of CSDS-Fe, CSDS-P, CSDS-P-Fe and CSDS-P-I hydrogels with the surrounding tissue after 5 days, 10 days and 15 days of implantation in subcutaneous tissue of ICR mice. Epidermis (E), Hair fossil (F), scab (S), Adipose layer (A), Hydrogels or the contacting sections (H or *). The nucleus and the ribosomes stained purple-blue, and the cytoplasm and the extracellular matrix stained red by H&E.

cytoplasm, are emigrated from the blood vessels and accumulated in the surrounding tissues of the hydrogels, indicating a minor local host inflammatory response, and CSDS-Fe showed more inflammatory cells around it than the double cross-linked hydrogels. After 10 days of implantation, inflammatory cells were increasing and infiltrated into the hydrogels due to the degradation of the implanted hydrogels. After 15 days of implantation, these inflammatory cells were significant reducing, it has demonstrated the disappearance of the inflammatory reaction. Additionally, the collagens were deposited, which confirmed by the Masson's trichrome staining (Fig. S9, Supporting Information). Therefore, these results proved the biodegradability and biocompatibility *in vivo* of the mussel inspired double-cross-linked hydrogels.

4. Conclusions

Inspired by the high adhesive and synergistic effects of mfps, in this study, we designed and prepared an injectable double cross-linked hydrogel adhesive composed of CSDS and PEG-4S by the sequential two-step reaction. CSDS with catechol groups and thiol groups and PEG-4S were successful synthesized and they were rapidly formed double cross-linked networks by adding the fast cross-linker. The mechanical and adhesion properties were enhanced due to the synergistic effects of the functional groups. Furthermore, it was demonstrated that the adhesion was promoted by controlling the redox reaction between the reactive groups. The results of subcutaneous implantation proved that the double cross-linked hydrogel was biodegradable and biocompatible. This research provides a potential hydrogel adhesive for biomedical application.

CRediT authorship contribution statement

Zhiwen Zeng: Investigation, Conceptualization, Data Curation, Writing-Original Draft, Project administration, Writing-Review & Editing. **Dinghua Liu**: Data Curation, Visualization, Animal Model. **Dejian Li**: Data Curation, Resources, Animal Model. **Xiumei Mo**: Conceptualization, Methodology, Writing-Original Draft, Supervision, Project administration, Funding acquisition, Writing-Review & Editing.

Declaration of Competing Interest

The authors report no declarations of interest.

Acknowledgements

This research was supported by National Key Research Program of China (2016YFA0201702 of 2016YFA0201700), National Nature Science Foundation of China (Nos.31470941, 31771023), Science and Technology Commission of Shanghai Municipality (Nos.15JC1490100, 15441905100), Yantai Double Hundred Talent Plan, and "111 Project" Biomedical Textile Materials Science and Technology, China (No. B07024).

Appendix A. Supplementary data

Supplementary material related to this article can be found, in the online version, at doi:https://doi.org/10.1016/j.colsurfb.2021.111782.

References

[1] R. Pinnaratip, M.S.A. Bhuiyan, K. Meyers, R.M. Rajachar, B.P. Lee, Multifunctional biomedical adhesives, Adv. Healthc. Mater. 8 (2019), e1801568.
[2] M.E. Parente, A. Ochoa-Andrade, G. Ares, F. Russo, A. Jimenez-Kairruz, Bioadhesives hydrogels for cosmetic application, Int. J. Cosmet. Sci. 37 (2015) 511–518.
[3] A. Meddahi-Pelle, A. Legrand, A. Marcellan, L. Louedec, D. Letourneur, Leibler L. Organ Repair, Hemostasis, and *in vivo* bonding of medical devices by aqueous solutions of nanoparticles, Angew. Chemie 53 (2014) 6369–6373.
[4] J. Li, A.D. Celiz, J. Yang, Q. Yang, I. Wamala, W. Whyte, et al., Tough adhesives for diverse wet surfaces, Science 357 (2017) 378–381.
[5] R. Cui, F. Chen, Y. Zhao, W. Huang, C. Liu, A novel injectable starch-based tissue adhesive for hemostasis, J. Mater. Chem. B 8 (2020) 8282–8293.
[6] Y. Zhang, C. Tang, P.N. Span, A.E. Rowan, T.W. Aalders, J.A. Schalken, et al., Polyisocyanide hydrogels as a tunable platform for mammary gland organoid formation, Adv. Sci. 7 (18) (2020), 2001797.

[7] C. Xie, X. Wang, H. He, Y. Ding, X. Lu, Mussel-inspired hydrogels for self-adhesive bioelectronics, Adv. Funct. Mater. 30 (2020), 1909954.
[8] M.G. Mazzotta, A.A. Putnam, M.A. North, J.J. Wilker, Weak bonds in a biomimetic adhesive enhance toughness and performance, J. Am. Chem. Soc. 142 (2020) 4762–4768.
[9] P. Rao, T.L. Sun, L. Chen, R. Takahashi, G. Shinohara, H. Guo, et al., Tough hydrogels with fast, strong, and reversible underwater adhesion based on a multiscale design, Adv. Mater. 30 (2018), e1801884.
[10] H. Yi, M. Seong, K. Sun, I. Hwang, K. Lee, C. Cha, et al., Wet-responsive, reconfigurable, and biocompatible hydrogel adhesive films for transfer printing of nanomembranes, Adv. Funct. Mater. 28 (2018), 1706498.
[11] P.L. Thi, Y. Lee, D.H. Nguyena, K.D. Park, In situ forming gelatin hydrogels by dual-enzymatic cross-linking for enhanced tissue adhesiveness, J. Mater. Chem. B 5 (2017) 757–764.
[12] P. Kord Forooshani, B.P. Lee, Recent approaches in designing bioadhesive materials inspired by mussel adhesive protein. Journal of polymer science part a, Polym. Chem. 55 (2017) 9–33.
[13] H. Jung, M.K. Kim, J.Y. Lee, S.W. Choi, J. Kim, Adhesive hydrogel patch with enhanced strength and adhesiveness to skin for transdermal drug delivery, Adv. Funct. Mater. 30 (42) (2020), 2004407.
[14] F. Pan, S. Ye, R. Wang, W. She, J. Liu, Z. Sun, et al., Hydrogel networks as underwater contact adhesives for different surfaces, Mater. Horiz. 7 (2020) 2063–2070.
[15] X. Fan, W. Zhou, Y. Chen, L. Yan, Y. Fang, H. Liu, An Antifreezing/Antiheating hydrogel containing catechol derivative urushiol for strong wet adhesion to various substrates, ACS Appl. Mater. Interfaces 12 (2020) 32031–32040.
[16] Y. Liu, H. Meng, S. Konst, R. Sarmiento, R. Rajachar, B.P. Lee, Injectable dopamine-modified poly(ethylene glycol) nanocomposite hydrogel with enhanced adhesive property and bioactivity, ACS Appl. Mater. Interfaces 6 (2014) 16982–16992.
[17] J.J. Wilker, Positive charges and underwater adhesion, Science 349 (2015) 582–583.
[18] C. Chai, Y. Guo, Z. Huang, Z. Zhang, S. Yang, W. Li, et al., Antiswelling and durable adhesion biodegradable hydrogels for tissue repairs and strain sensors, Langmuir 36 (2020) 10448–10459.
[19] B.J. Kim, D.X. Oh, S. Kim, J.H. Seo, D.S. Hwang, A. Masic, et al., Mussel-mimetic protein-based adhesive hydrogel, Adv. Mater. 28 (2016) 8675–8680.
[20] S. Hong, D. Pirovich, A. Kilcoyne, C. Huang, H. Lee, R. Weissleder, Supramolecular metallo-bioadhesive for minimally invasive use, Biomaterials 35 (2014) 711–719.
[21] M. Mehdizadeh, H. Weng, D. Gyawali, L. Tang, J. Yang, Injectable citrate-based mussel-inspired tissue bioadhesives with high wet strength for sutureless wound closure, Biomaterials 33 (2012) 7972–7983.
[22] J.D. White, J.J. Wilker, Underwater bonding with charged polymer mimics of marine mussel adhesive proteins, Macromolecules 44 (2011) 5085–5088.
[23] J. Yu, W. Wei, E. Danner, R.K. Ashley, J.N. Israelachvili, J.H. Waite, Mussel protein adhesion depends on interprotein thiol-mediated redox modulation, Nat. Chem. Biol. 7 (2011) 588–590.
[24] J. Yu, W. Wei, E. Danner, J.N. Israelachvili, J.H. Waite, Effects of interfacial redox in mussel adhesive protein films on Mica, Adv. Mater. 23 (2011) 2362–2366.
[25] Q. Lu, D.X. Oh, Y. Lee, Y. Jho, D.S. Hwang, H. Zeng, Nanomechanics of Cation-π interactions in aqueous solution, Angew. Chemie 52 (2013) 3944–3948.
[26] S. Bai, X. Zhang, X. Lv, M. Zhang, X. Huang, Y. Shi, et al., Bioinspired mineral–Organic bone adhesives for stable fracture fixation and accelerated bone regeneration, Adv. Funct. Mater. 30 (2019), 1908381.
[27] M.S. Desai, M. Chen, F.H.J. Hong, J.H. Lee, Y. Wu, S.W. Lee, Catechol-functionalized elastin-like polypeptides as tissue adhesives, Biomacromolecules 21 (2020) 2938–2948.
[28] L. Han, M. Wang, L.O. Prieto-López, X. Deng, J. Cui, Self-hydrophobization in a dynamic hydrogel for creating nonspecific repeatable underwater adhesion, Adv. Funct. Mater. 30 (2019), 1907064.
[29] Y. Zhou, W. Nie, J. Zhao, X. Yuan, Rapidly in situ forming adhesive hydrogel based on a PEG-Maleimide modified polypeptide through michael addition, J. Mater. Sci. Mater. Med. 24 (2013) 2277–2286.
[30] C. Lurtz, K. Voss, V. Hahn, F. Schauer, J. Wegmann, E.K. Odermatt, et al., *In vitro* degradation and drug release of a biodegradable tissue adhesive based on functionalized 1,2-ethylene glycol bis(dilactic acid) and chitosan, J. Mater. Sci. Mater. Med. 24 (2013) 667–678.
[31] D-y Teng, Z-m Wu, X-g Zhang, Y-x Wang, C. Zheng, Z. Wang, et al., Synthesis and characterization of in situ cross-linked hydrogel based on self-assembly of thiol-modified chitosan with PEG diacrylate using Michael type addition, Polymer 51 (2010) 639–646.
[32] W. Nie, X. Yuan, J. Zhao, Y. Zhou, H. Bao, Rapidly in situ forming Chitosan/Epsilon-Polylysine hydrogels for adhesive sealants and hemostatic materials, Carbohydr. Polym. 96 (2013) 342–348.
[33] Z. Zeng, X. Mo, Rapid in situ cross-linking of hydrogel adhesives based on thiol-grafted bio-inspired catechol-conjugated chitosan, J. Biomater. Appl. 32 (2017) 612–621.
[34] Z. Zeng, X.M. Mo, C. He, Y. Morsi, H. El-Hamshary, M. El-Newehy, An in Situ Forming Tissue Adhesive Based on Poly(ethylene glycol)-Dimethacrylate and Thiolated Chitosan Through the Michael Reaction, J. Mater. Chem. B 4 (2016) 5585–5592.
[35] E.A. Phelps, N.O. Enemchukwu, V.F. Fiore, J.C. Sy, N. Murthy, T.A. Sulchek, et al., Maleimide cross-linked bioactive PEG hydrogel exhibits improved reaction kinetics and cross-linking for cell encapsulation and in situ delivery, Adv. Mater. 24 (2012) 64–70.
[36] P. Karami, C.S. Wyss, A. Khoushabi, A. Schmocker, M. Broome, C. Moser, et al., Composite double-network hydrogels to improve adhesion on biological surfaces, ACS Appl. Mater. Interfaces 10 (2018) 38692–38699.
[37] F. Lin, Z. Wang, J. Chen, B. Lu, L. Tang, X. Chen, et al., A bioinspired hydrogen bond crosslink strategy toward toughening ultrastrong and multifunctional nanocomposite hydrogels, J. Mater. Chem. B 8 (2020) 4002–4015.
[38] T. Miron, M. Wilchek, A simplified method for the preparation of succinimidyl carbonate polyethylene glycol for coupling to proteins, Bioconjug. Chem. 4 (1993) 568–569.
[39] J.H. Waite, C.V. Benedict, Assay of dihydroxyphenylalanine (Dopa) in invertebrate dtructural proteins, Meth. Enzymol. 107 (1984) 397–413.
[40] K. Kim, J.H. Ryu, D.Y. Lee, H. Lee, Bio-inspired catechol conjugation converts water-insoluble chitosan into a highly water-soluble, adhesive chitosan derivative for hydrogels and LbL assembly, Biomater. Sci. 1 (2013) 783–790.
[41] D.X. Oh, S. Kim, D. Lee, D.S. Hwang, Tunicate-mimetic nanofibrous hydrogel adhesive with improved wet adhesion, Acta Biomater. 20 (2015) 104–112.
[42] H. Meng, Y. Li, M. Faust, S. Konst, B.P. Lee, Hydrogen peroxide generation and biocompatibility of Hydrogel-Bound Mussel adhesive moiety, Acta Biomater. 17 (2015) 160–169.
[43] J. Deng, Y. Tang, Q. Zhang, C. Wang, M. Liao, P. Ji, et al., A bioinspired medical adhesive derived from skin secretion of Andrias davidianus for wound healing, Adv. Funct. Mater. 29 (2019), 1809110.